Benchmarking on improvement and site-adaptation techniques for modeled solar radiation datasets

Jesus Polo[1], Carlos Fernández-Peruchena[2], Vasileios Salamalikis[3], Luis Mazorra-Aguiar[4], Mathieu Turpin[5], Luis Martín-Pomares[6], Andreas Kazantzidis[3], Philippe Blanc[7], Jan Remund[8]

[1] Photovoltaic Solar Energy Unit (Energy Department e CIEMAT), Avda. Complutense 40, 28040 Madrid, Spain

[2] Spanish Center of Renewable Energies (CENER), Spain

[3] Laboratory of Atmospheric Physics, University of Patras, Greece

[4] SIANI, University of Las Palmas de Gran Canaria, Spain

[5] Reuniwatt SAS, 14 rue de la Guadeloupe, 97490 Sainte-Clotilde, France

[6] ISES member, PVPS-Task 16 participant

[7] Center O.I.E. Mines ParisTech Armines, France

[8] Meteotest, Fabrikstrasse 14, CH-3012 Bern, Switzerland

Corresponding Author:

Jesús Polo, email: jesus.polo@ciemat.es , Phone: +34 914952513, Fax : +34 913466037

Abstract

High-accuracy solar radiation data are needed in almost every solar energy project for bankability. Time series of solar irradiance components that spans decades can be supplied by satellite-derived irradiance or by reanalysis models, with very various types of uncertainty associated to the specific approaches taken and quality of boundary conditions information. In order to improve the reliability of these modeled datasets, comparison with ground measurements over a short period of time can be used for correcting some aspects, bias mainly, of the modeled data by using different methodologies; this procedure is known as site adaptation. Therefore, a benchmarking exercise that uses different site adaptation techniques was proposed within the Task 16 IEA-PVPS activities. In this work, over ten different site-adaptation techniques have been used for assessing the accuracy improvement, using ten different datasets covering both satellite-derived and reanalysis solar radiation data. The effectiveness of these methods is found not universal or spatially homogeneous, but in general, it can be stated that significant improvements can be achieved eventually in most sites and datasets.

This document is the Accepted Manuscript version of a Published Work that appeared in final form in Solar Energy. To access the final edited and published work see [10.1016/j.solener.2020.03.040

Keywords: satellite-derived solar radiation, site adaptation, bankability of data for solar projects, modeled solar radiation data

1. Introduction

Solar power deployments, such as photovoltaics (PV) or concentrating solar power (CSP) plants, require high-quality decade-long time series of solar radiation data for both technical (planning dimensioning and designing stages) and financial aspects of the project. The long-term variability of solar resources plays a significant role in estimating the probability of exceedance of the future energy yields of a solar power plant, and it influences the financial conditions that the project is likely to receive (Fernández-Peruchena et al., 2018). Notwithstanding, due to the significant intra-day and inter-annual variability of solar irradiance, the solar resource assessment should consider time series, instead of only considering the climatological averages. Reliable and bankable solar radiation data should include at least time series of direct normal irradiance (DNI) for CSP projects, and global horizontal irradiance (GHI) or plane of array (POA) global irradiance for the PV ones (Sengupta et al., 2017). Additionally, high-quality diffuse horizontal irradiance (DHI) data are also desirable and might be required in specific solar projects and applications.

Long-term time series of the solar radiation components at the Earth's surface can be modelled by many methodologies based on satellite imagery or numerical weather model reanalysis. The use of satellite-based models is currently most common in carrying out both solar resource mapping and site-specific solar irradiance data generation, since this approach has achieved a high degree of maturity and reliability. Solar engineers' extensive modeling experience in producing operational satellite-derived irradiance can be traced back to the late 1980s (Cano et al., 1986; Polo et al., 2008; Polo and Perez, 2019). The works that aim to validate, improve and apply these satellite-based methods are still on-going today and are being reported regularly in the relevant scientific and industry communities (Cros et al., 2019; Merrouni et al., 2017; Perez et al., 2017; Pfeifroth et al., 2017; Porfirio and Ceballos, 2017; Qu et al., 2017; Riihelä, 2018; Tang et al., 2016; Thomas et al., 2016; Urraca et al., 2017; Yang, 2019, 2018; Yang and Boland, 2019; Yang and Perez, 2019). High-quality, satellite-derived irradiance datasets are made freely available by several providers, such as PVGIS (Amillo et al., 2014), CM-SAF (Kothe et al., 2019; Posselt et al., 2012), or NSRDB (Sengupta et al., 2018). In addition, the quality of the latest reanalysis data has improved significantly (Urraca et al., 2018), although the specific validation exercise was performed using daily data and the hourly results are still unclear. Nevertheless, large number of recent works highlights the interest on this topic (Feng and Wang, 2019; Huld et al., 2018; Peng et al., 2019; Perdigão et al., 2016; Ramirez Camargo and

Dorner, 2016; Salazar et al., 2020; Tahir et al., 2020; Trolliet et al., 2018; Zib et al., 2012).

That said, despite the improvements and quality gained in the recent years, various types of uncertainties are still embedded in modeled solar irradiance datasets, particularly owing to the uniformity of the data-generating process. Stated differently, when a model retrieves solar irradiance at a specific site some uncertainties are involved. Systematic errors in the models, limitations in the spatial and temporal resolutions, uncertainty in the atmospheric data that affects the radiative transfer process are, among others, some of the major sources of uncertainty that can result in biases or deviations in the modeled data.

Validation results in the literature for GHI and DNI, either satellite-derived or reanalysis-based, are very difficult to summarize. A huge amount of studies can be found elsewhere. Many providers and models report uncertainties that can vary a lot depending on the geographic area, the intrinsic characteristics of the model and on the quality of ground data used for validation. In order to illustrate this variability, just a few recent validation results are given next. Uncertainties in the range of -4 to 9% MBD (Mean Bias deviation) and 17-50% RMSD (Root Mean Square Deviation) for hourly GHI were reported with the eastern Meteosat satellite (Amillo et al., 2014). In India, SARAH-E satellite-based estimations resulted in 10-20% overestimation of the surface incoming solar radiation (Riihelä, 2018). In Chile, nearly unbiased hourly GHI with 20% RMSD was recently estimated using GOES satellite imagery (Molina et al., 2017). Recent validation of the National Solar Radiation database (NSRBD) reported RMSD ranges of 9-18% and 15-30% for hourly GHI and DNI, respectively (Yang, 2018). The HelioClim-3 database reported 8% MBD and 20% RMSD for DNI estimations in Morocco (Merrouni et al., 2017). Version 4 of the SUNY model has improved notably its performance in both GHI and DNI (Perez et al., 2015). Therefore, quality, availability and completeness of the ground data, topography and climatology of the site, accuracy of the boundary conditions and input parameters (atmospheric composition, cloud properties, etc.) play an important role in the uncertainty characterization of the models for estimating solar radiation components.

In virtually every solar power project, and in many other applications, the preliminary characterization of long-term solar resources is done by evaluating the modeled time series of solar irradiance against short-term local ground measurements. Setting up a high-quality, ground-based monitoring station at the project site is always recommended for projects with significant financial investment. It is also highly recommended to keep the station instruments properly calibrated and maintained. The assessment of long-term data by comparing to local measurements could help in terms of uncertainty quantification and mitigating the financing risk of the project

(Armansperg et al., 2015; Fernández-Peruchena et al., 2018; Fernández Peruchena et al., 2016; Guerreiro et al., 2016; Hirsch et al., 2017; Meyer and Schwandt, 2017; Polo et al., 2017, 2016a; Richter et al., 2015). Moreover, a reasonable period of ground measurements (usually a year) can be used to remove bias, and thus correct and improve the long-term solar radiation time series by different techniques. These techniques aim to find a relationship between the ground and modeled data that can be extrapolated to the past, as a means for minimizing the statistical deviations. This process of calibration or correction of modeled data by including observational data has been used in the retrievals of other meteorological variables (wind velocity, precipitation, etc.). In the field of energy meteorology, such correction procedures have been frequently termed *site adaptation* techniques (Polo et al., 2016b). Several example techniques that have been applied to improve the goodness of solar radiation time series can be found in the recent literature (Frank et al., 2018; Mazorra Aguiar et al., 2019; Perez et al., 2010; Polo et al., 2015; Tahir et al., 2020).

In the framework of the Task 16 of IEA-PVPS (http://www.iea-pvps.org/index.php?id=389) and Task V of IEA-SolarPACES entitled “Solar Resource for High Penetration and Large Scale Applications”, several activities are being addressed in benchmarking, models assessment and improving knowledge of modeling solar radiation components. Improvement in measuring protocols, gap filling, and quality check of ground data and benchmarking of models are, among others, activities focused on improving the bankability of solar radiation products. In this context, benchmarking and reviewing of site-adaptation techniques for solar resource data are stated as activities of interest (Remund et al., 2017). Under this framework, several task participants are developing different techniques and procedures for improving and correcting the modeled datasets, for various satellite-derived and reanalysis datasets, in order to have a sample of modeled solar radiation data that can typify the different types of uncertainties.

A first benchmarking exercise has been developed by four teams of scientists, and its methodology and results are reported here. Each team has implemented one or several site adaptation techniques, according to their previous experience and skills. All these methodologies have been applied in a blind exercise to 10 different datasets (consisted of pairs of ground and model sets of data of the solar irradiance components: GHI, DNI and DHI).

For the present needs, a blind exercise is justified to protect some of the techniques that are, or could be become, commercial. This study aims at performing a pure statistical exercise to explore the capability of a given technique to improve a dataset using a small part of the observations. Therefore ground and model datasets, and techniques, are selected following these simple rules: covering quite different climates, using mostly free and open-source modeled and ground data, and selecting those site adaptation techniques with enough details in the literature for easy implementation. This paper acts as a report for those findings.

2. Description of the methodologies and approaches

Different methodologies have been tested in this work for site adaptation of solar radiation data. Some of them originate from other subdomain of meteorology (Piani et al., 2010; Wilcke et al., 2013). This section provides a general description of the fundamentals of those methodologies considered in this work. It is emphasized that more site adaptation techniques do exist, and some of them were described in Polo et al. 2016; hence, the present contribution should not be considered exhaustive. The procedures for using these techniques can be applied to either the entire dataset, or subsets of data that are divided according to solar elevation or sky classification, for instance. In order to emulate a realistic situation in resource assessment for solar projects, each site-adaptation procedure has been carried out using data from the latest year available at each site, and each adapted series has been compared with measured data spanning the entire history of that site.

2.1 Linear regression bias removal

The bias removal using a linear regression model aims at finding a linear relationship between the measured and modeled data, which often can result in an improved coefficient of determination of the pair of random variables. This simple methodology is quite commonly used to correct satellite-derived solar radiation data, showing good results in presence of large seasonal bias (Mazorra Aguiar et al., 2019; Polo et al., 2016b, 2015). Linear least squares fitting is performed between the modeled data (x_m) and observations (x_o) over a selected period of time (e.g., one year) to obtain the slope (a) and the y-intercept (b). The bias-removal procedure for the fitting data can be expressed using the following equation:

$$y = x_m - [(\mathrm{a}-1)\, x_o + b]. \tag{1}$$

Such expression of y and x_m results in a linear function f that can be used to transform all the historical modeled data into new corrected data, y_c.

$$y_c = f(x_m), \tag{2}$$

where f represents the linear function resulting from fitting the corrected y_c values versus the original y. This procedure has similarities with the Measured-Correlated-

Predict (MCP) methods (Carta et al., 2013). In the context of this work this method will be called LIN-FIT for better comparison with the other methodologies used here.

2.2 Quantile mapping (QM)

The quantile mapping (QM) technique has been employed in climate modeling and meteorology for correcting the distribution of a modeled parameter by comparing it against the empirical distribution of the observations (Déqué et al., 2007; Ines and Hansen, 2006). The approach seeks to transform the data to a probability domain (quantiles) and applies the inverse transformation using the cumulative distribution function (CDF) of the observational data to obtain the corrected data (Déqué et al., 2007),

$$y_c = \mathrm{CDF}_o^{-1}[\mathrm{CDF}_m(x_m)], \tag{3}$$

where CDF_o and CDF_m are the cumulative distribution functions of the observed and modeled data, respectively.

The quantiles of modeled and observed data can be computed by the full empirical non-parametric distribution or by a fitted theoretical parametric distribution (Feigenwinter et al., 2018; Piani et al., 2010; Themeßl et al., 2012).

2.3 Quantile delta mapping (QDM)

The quantile delta mapping (QDM) bias-correction method is an extension of the conventional QM technique (Cannon, 2018; Cannon et al., 2015). The algorithm preserves the model-projected relative changes in quantiles, and additionally, corrects the systematic quantile biases of the modeled data with respect to the observed values. The bias-adjustment of the modeled values for the reference period is the same as the traditional QM technique. With respect to the target variable, two corrections are applied (additive and multiplicative):

$$y_c = x_m + \mathrm{CDF}_o^{-1}[\mathrm{CDF}_m(x_m)] - \mathrm{CDF}_m^{-1}[\mathrm{CDF}_m(x_m)], \tag{4}$$

$$y_c = x_m \frac{\mathrm{CDF}_o^{-1}[\mathrm{CDF}_m(x_m)]}{\mathrm{CDF}_m^{-1}[\mathrm{CDF}_m(x_m)]}\ .$$

2.4 Cumulative distribution function-transform (CDF-T)

The CDF-T method performs QM based on the CDFs over the future period, thus, allowing the CDF to change with respect to the reference period. It provides an extension of the traditional QM method since the QM technique only transforms the modeled values of the future period onto the CDF of the reference period (Michelangeli et al., 2009).

2.5 Kernel density distribution mapping (KDM)

Kernel density distribution mapping (KDM) method uses a similar logic as QM, at least algorithmically. In general, QM enables the bias-adjustment by transforming the modeled values into quantiles, and then projecting them into data values in terms of the quantile function (inverse CDF) of the observations (McGinnis et al., 2015). In KDM the CDF and the CDF^{-1} functions are expressed in terms of the kernel density estimator. The probability density functions (PDF) of the modeled and the observed values are estimated non-parametrically using kernel density estimation assuming a Gaussian kernel (Izenman, 2016). Two slightly different versions of KDM have been used in this work. KDM-T and KDM-CS refer to the application of the technique to the whole dataset and to subsets according to sky conditions (clear or non-clear), respectively. KDMR is just KDM with an optimal bandwidth algorithm.

2.6 Site-specific multiple regression (SIM)

This method is based on the multi-model inference (also known as ensemble) of multiple linear regression models, through computing, comparing, and ranking an exhaustive list of models. For the local adaptation of GHI, an exhaustive screening of the selected exogenous variables is carried out, followed by a selection of a best model as per the Akaike information criterion (AIC). The model is constructed through both the selected variables and their interactions; the exogenous variables include clearness index of modeled GHI series (*Kt*, the ratio of GHI to top-of-atmosphere solar irradiance on the same plane); relative air mass (*m*); modeled clear-sky index (*Kc*, the ratio between modeled GHI and its corresponding value under clear-sky conditions); and solar elevation angle. The clear-sky model used in this method is McClear (Lefèvre et al., 2013), available through the Copernicus Atmosphere Monitoring Service (CAMS, http://www.soda-pro.com/web-services/radiation/cams-mcclear).

The methodology for the local adaptation of DNI is based on the previous adaptation of the diffuse horizontal irradiance (DHI), because the ratio DHI to GHI (K, diffuse fraction) is known to be reliably predictable from the following parameters (and their combinations): *m*, *Kc*, solar elevation, and a fourth-order polynomial of Kt_m. Finally, DNI is calculated from both locally adapted GHI and DHI by the closure equation, assuring the accomplishment of the fundamental relations between these solar radiation components. Finally, the procedure is applied separately for clear-sky and non-clear-sky days.

2.7 Sequential regressive-quantile mapping procedure (SIMEQ)

This method is a sequential application of two procedures of different nature. Firstly, the SIM technique (described in the preceding subsection, 2.6) is applied, which is based on the multimodel inference of multiple linear regression models. Secondly, a bias correction based on empirical quantile mapping (eQM) is applied on both GHI and DNI adapted series. This method consists in calibrating the simulated CDF by adding to the observed quantiles both the mean delta change and the individual delta changes in the corresponding quantiles. Finally, DHI is calculated from the locally adapted GHI and DNI, through the closure equation, thus satisfying the fundamental relations between these solar radiation components.

The first procedure (i.e., the SIM method) can considerably reduce both the dispersion and the deviation in CDF of the adapted solar irradiance series, with respect to the modeled ones. The application of the second procedure (eQM) to the mentioned adapted series significantly reduces the deviation in CDF, while maintaining or reducing the values of the dispersion statistical indicators. Similar to the case of the SIM technique, this procedure is applied separately to clear and non-clear-sky days.

2.8 Regressions using subsets of data

Specific regressions and fitting techniques can be also applied to subsets of data as a site adaptation procedure. In this paper a methodology is used for correcting only GHI where subsets of ground and modeled data are first classified into different ranges of solar zenith angles and clear-sky index, K_{cs} (the ratio between the modeled GHI and its corresponding value under clear-sky conditions). Solar zenith angles are divided into 5 groups in the range of 0-75° with intervals of 15°, whereas K_{cs} is divided into two groups, namely lower and greater than 0.55. For each combination of groups (10 combinations in total), a pair of third-degree polynomial regressions are applied to the last year of modeled and ground data - one for GHI and the other one for K_{cs}. Moreover, two additional regressions (again one for GHI and one for K_{cs}) are calculated from samples of the entire year (solar zenith angle between 0-75° and K_{cs} between 0 and 1). This makes a total of 22 regressions. The one that minimizes the relative bias is picked for this particular subsample.

3. Ground and modeled datasets

In order to benchmark the different site adaptation techniques, sites are selected from locations under different climates, and covered by different networks of ground stations. In addition, different types of modeled data (i.e., satellite-derived and reanalysis) are used. Most of these data belong to different satellite-derived datasets, estimated using different methods, and issued by various providers. Reanalysis data, on the other hand, cover two high-latitude sites, where satellite images do not resolve. Table 1 summarizes the metadata of the selected sites, which are drawn on the world map together with their climatic types in Figure 1. In this regard, the datasets herein used belong to modeled data with very different uncertainties corresponding to two different reanalyses, several satellite models with different approaches regarding the clear-sky transmittance, atmospheric information (aerosol optical depth or turbidity, water vapor and other components) and satellite imagery (different satellite platforms). Each dataset contains both the modeled and measured hourly values of the three basic solar radiation components (GHI, DNI and DHI). In addition, some, but not all, BSRN-recommended quality checks for ground data are performed (Long and Dutton, 2004), for both ground and model data. The reason is to allow the assessment of site adaptation methods as a "blind" statistical tool attempting to fit different model data to observational ones.

Table 1. Summary of sites with pair ground-model datasets for benchmarking

Site (code)	**Latitude (°N)**	**Longitude (°E)**	**Elevation (m)**	**Climate**	**Period**	**Model type**
Alice Springs (ASP)	-23.79	133.88	547	Hot desert, arid	2007-2013	Satellite
Boulder (BOU)	40.12	-105.23	1689	Cold semi-arid	2009-2015	Satellite
Tateno (TAT)	36.05	140.12	25	humid subtropical	2009-2015	Satellite
Tamanrasset (TAM)	22.79	5.52	1385	Hot desert, arid	2007-2011	Satellite
Carpentras (CAR)	44.08	5.05	100	Mediterranean	2007-2013	Satellite
Burns (BRN)	43.52	-119.02	1271	Cold semi-arid	2007-2013	Satellite
Kiruna (KIR)	67.48	20.41	424	subarctic	2008-2014	Reanalysis
Norrköping (NRK)	58.58	16.14	53	humid continental	2008-2014	Reanalysis
Visby (VIS)	57.67	18.34	49	oceanic	2008-2014	Satellite
Sede Boqer	30.86	34.77	500	Hot desert, arid	2006-2011	Satellite

4. Deviations of the model datasets

The evaluation approach for the modeled datasets is described before presenting the results of the different site adaptation techniques. For assessment of model and site adaptation performance, three metrics are selected: mean bias deviation (MBD), root mean square deviation (RMSD) and Kolmogorov-Smirnov integral (KSI). The first two accuracy measures indicate bias and dispersion, whereas the third informs the similitude of CDFs of modeled and measured data (Gueymard, 2014). Table 2 shows the statistical metrics expressed in percent of all the modeled datasets (i.e. the original uncorrected datasets as delivered by the different models used) for the three components. Large ranges of bias, dispersion and similitude of distribution functions in the model dataset can be observed as a consequence of taking both the site characteristics and the approaches into account in the modeling. This is a good outcome from the study since the scope of this work is not the performance of models retrieving solar radiation data but the capability of statistical methods to correct any model according to short-term observational values.

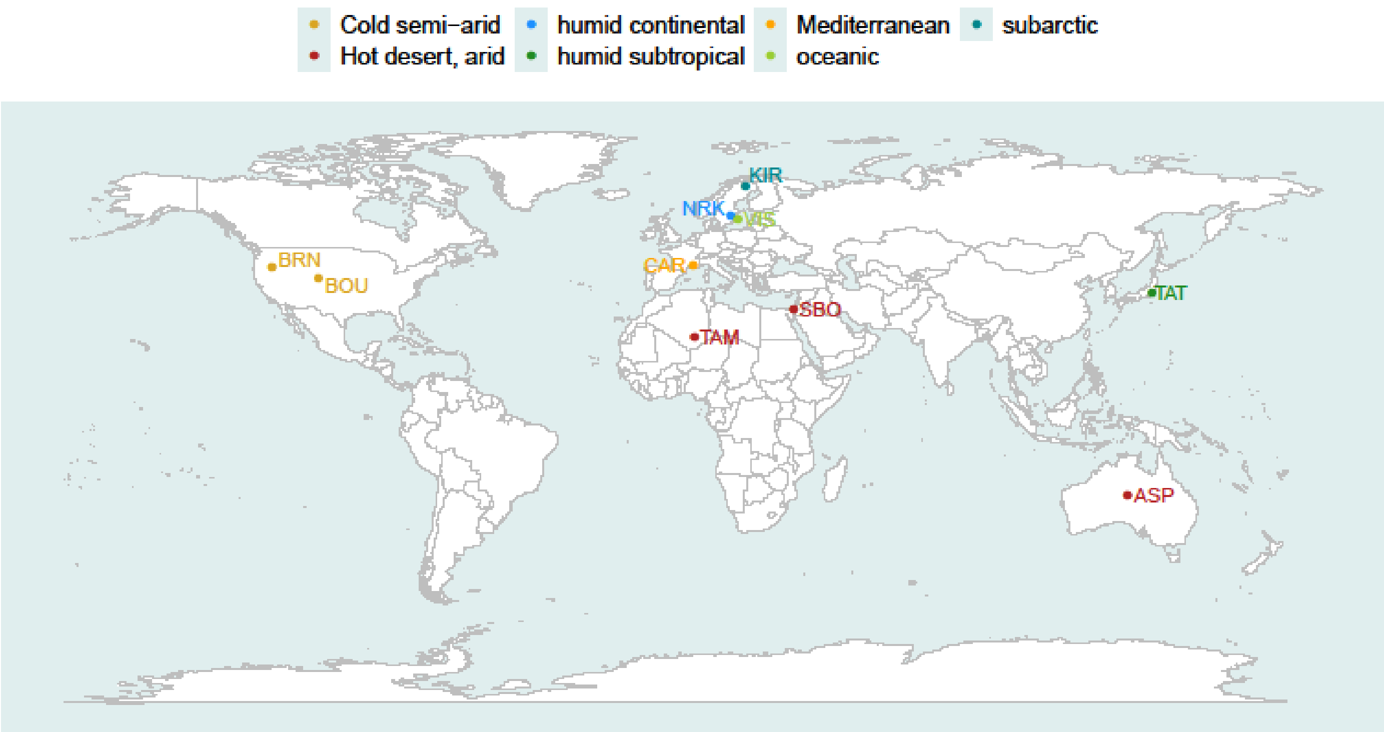

Figure 1. Sites selected for benchmarking site adaptation methods.

5. Site adaptation assessment results

Different procedures for site adaptation (up to 12) based on the previously described techniques (in Section 2) were used by four different teams in their attempt to generate corrected or improved values of the 10 datasets. Table 3 summarizes the characteristics of each procedure and details the team that employed each procedure. In all cases, the most recent year of ground data was used to train the model whereas the adaptation was applied to the whole period of the modeled dataset under scrutiny. It should be noted that eQM-CS and KDM-CS methods differ from other quantile mapping methodologies, since they are applied separately to the two subsets of modeled data that had been obtained for each sky condition (clear or non clear-sky). Therefore, prior to the use of those methods a selection of model data was done using an algorithm for automatic detection of clear-sky instants. In the case of eQM-CS and KDM-CS, the clear-sky detection is done using a method proposed by Gueymard 2013. The procedure requires DNI observations and concomitant DNI estimations under clear-sky conditions based on reliable aerosol optical depth (AOD) data. There is no perfect algorithm for a posteriori clear-sky identification in solar irradiance time series since any method may be affected by various sources of error, including inaccuracies in the input required. For instance, the computation of clear-sky components need of very accurate information of AOD and Precipitable water at least) (Gueymard, 2013; Gueymard et al., 2019). A very promising new model has been recently proposed in the literature for 1-min data (Bright et al., 2020). However the specific algorithm used in this work points the potential benefits of an accurate separation of clear and non clear-sky instants in site adaptation methodologies.

Table 2. Statistical metrics for the performance of uncorrected modeled datasets.

Site	**GHI (%)**			**DNI (%)**			**DHI (%)**		
	MBD	RMSD	KSI	MBD	RMSD	KSI	MBD	RMSD	KSI
Alice Springs	0.0	12.2	49.1	-1.1	20.1	203.7	3.2	47.1	127.1
Boulder	0.1	25.8	92.3	-6.1	49.9	102.6	9.7	50.6	99.3
Tateno	-3.3	18.3	46.9	-5.5	32.8	81.6	-1.3	31.2	117.6
Tamanrasset	-5.9	16.8	75.4	-12.7	38.8	223.7	9.8	51.7	206.8
Carpentras	2.6	17.4	50.1	3.6	31.5	64.7	3.7	42.0	144.9
Burns	-1.0	26.9	78.6	5.8	37.7	109.8	-9.6	60.1	247.6
Kiruna	106.9	258.3	31.1	39.4	179.7	23.3	26.8	141.6	37.7
Norrkoping	36.6	172.2	21.6	-18.6	118.5	18.7	33.9	141.7	43.4
Visby	33.1	170.2	28.6	-11.3	123.3	21.2	25.5	138.0	52.5
Sede Boqer	-3.9	33.7	75.1	-15.3	42.4	207.7	19.2	59.6	334.1

Table 3. Summary of site adaptation techniques and procedures.

Name	**Type**	**Components**	**Observations**	**Team**
eQM-T	Quantile Mapping	GHI,DNI,DHI	Empirical CDF	Team 1
eQM-CS	Quantile Mapping	GHI,DNI,DHI	Empirical CDF, separately to clear and non-clear-sky data	Team 1
KDM-T	Quantile Mapping	GHI,DNI,DHI	Kernel Density Distribution Mapping, limiting the maximum irradiance in the CDF to 5% over maximun observed	Team 1
KDM-CS	Quantile Mapping	GHI,DNI,DHI	Same as before but separately to clear and non-clear-sky data	Team 1
LIN-FIT	Regression	GHI,DNI,DHI	Simple linear fit	Team 2
CDF-T	Quantile Mapping	GHI,DNI,DHI	As described in section 2.4	Team 2

KDMR	Quantile Mapping	GHI,DNI,DHI	Kernel Density Distribution Mapping with optimal bandwidth	Team 2
QDM	Quantile Mapping	GHI,DNI,DHI	As described in section 2.3	Team 2
SIM	Multiple Regression	GHI,DNI,DHI	As described in section 2.6	Team 3
SIMEQ	Sequential	GHI,DNI,DHI	As described in section 2.7	Team 3
REG	Regression	GHI	As described in section 2.8	Team 4

Figures 2, 3 and 4 show the statistical metrics of the performance of the eight site adaptation methods for the GHI, DNI and DHI components, respectively. The first entry, referred to as model, indicates the original uncorrected modeled data in order to allow proper comparison and to illustrate the relative improvement in performance generated by each site adaptation method.

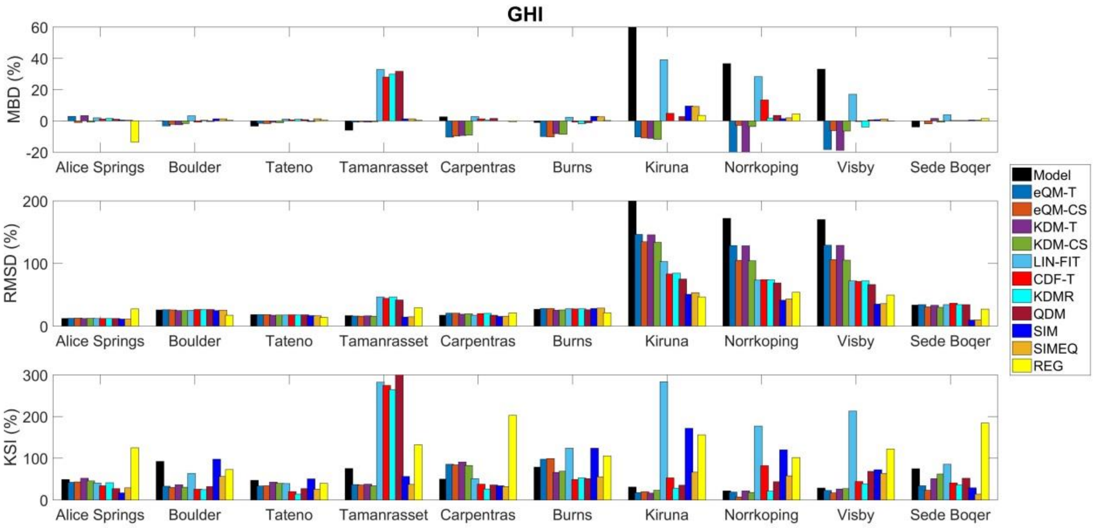

Figure 2. Statistical metrics for benchmarking of site adaptation applied to GHI.

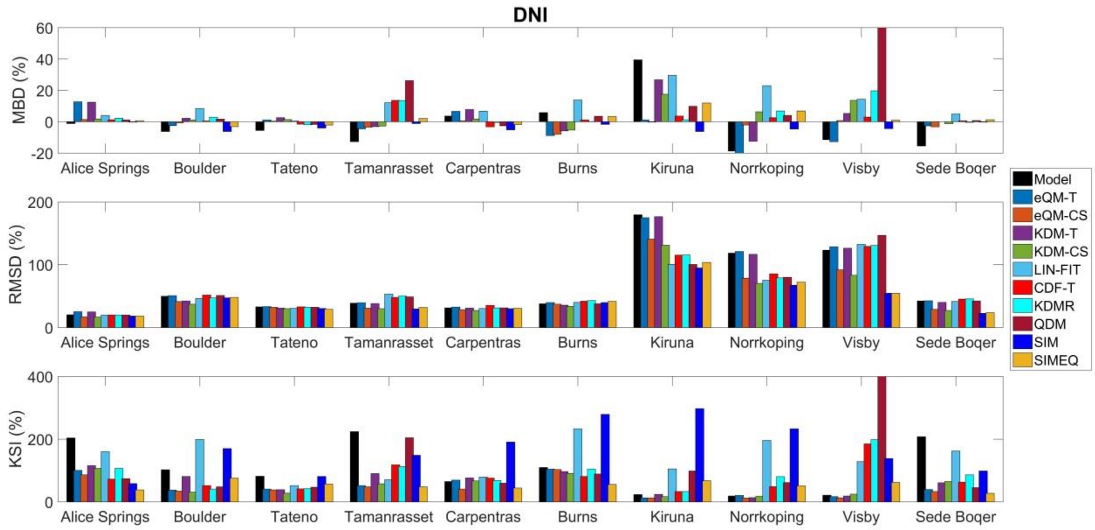

Figure 3. Statistical metrics for benchmarking of site adaptation applied to DNI.

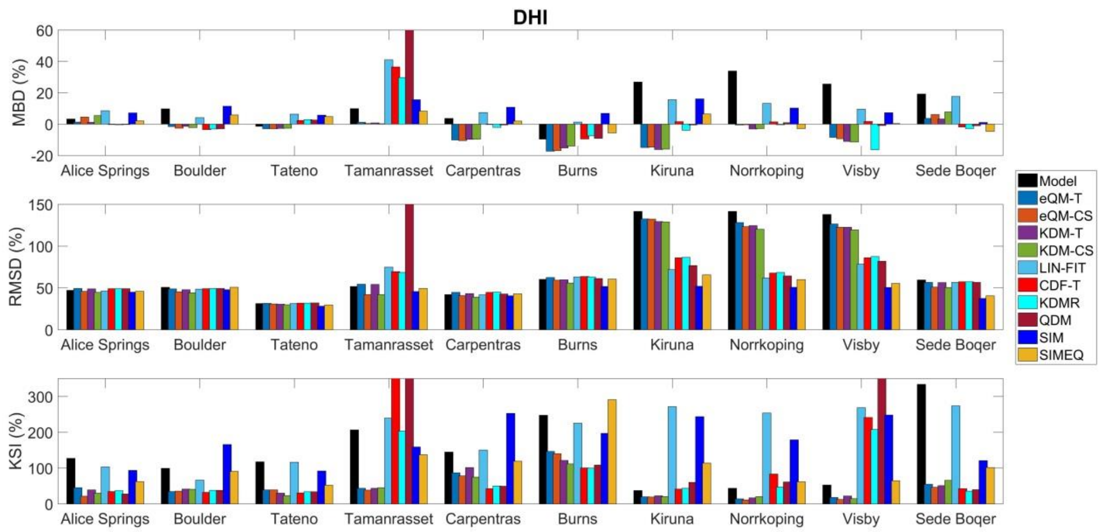

Figure 4. Statistical metrics for benchmarking of site adaptation applied to DHI.

The benchmarking results for GHI show that bias is not successfully removed in all cases. In particular, modeled datasets having an originally low bias (< 1%) site do not benefit from any improvement, with the exception of some QM-based (CDF-T, KDMR, QDM) and multiple regression based (SIM, SIMEQ) methods. However, in the case of modeled data with significant bias (> 30%), most techniques generally result in MBD improvement compared to unprocessed model data resulting in a much lower MBD (<10%) for most of them, and even in negligible bias (<1%) in the case of KDMR.

RMSD is very slightly improved by most techniques, except in the case of modeled datasets corresponding to the three sites (Kiruna, Norrkoping, and Visby) at very high latitude (>55°), where the original modeled data are affected by substantial uncertainty (Table 2), and where the site adaptation techniques induce a significant decrease in random errors. At those sites with the lowest RMSD values (< 20%), only those methods based on multiple regression (SIM, SIMEQ) achieved RMSD reduction (from 16.2% to 14.5%).

In the case of DNI, most of the methods are able to achieve significant improvement over the highly negatively biased modeled data (with typical MBD of ~15%), even bringing down the MBD to below 3% with some of them (eQM-CS, KDM-T, SIM and SIMEQ). The highly positively biased site (Kiruna, MBD = 39.5%) is satisfactorily corrected by some methods, among which eQM-T and eQM-CS should be highlighted. On the other hand, sites with moderate MBD (BOU and TAT, negatively bias at ~5.8%, and CAR and BRN, positively bias at ~4.8%) are satisfactorily corrected by most methods. Conversely, RMSD is more significantly improved by only some techniques. In particular, sites with high RMSD (KIR, NRK and VIS, with RMSD ~140%) are on average improved by all methods, among which SIM and SIMEQ should be highlighted because they reduce RMSD by half. At all other sites (typical RMSD ~36%), only some methods based both on QM (eQM-CS, KDM-T, KDM-CS) and multiple regression (SIM and SIMEQ) achieve improvements.

For the case of DHI, the situation at high-bias sites (MBD > 20%) is generally improved by the site adaptation techniques, whereas very different results are obtained at low-bias sites. Performance improvement in terms of RMSD is mainly observed for a few datasets wherever the initial bias is large.

On the other hand, there are some methods that eventually show a characteristic bad performance not observed at other sites. Thus, LIN-FIT, CDF-T, KDMR and QDM showed slightly or remarkable improvement in GHI and DHI except at Tamanrasset site. This particular behavior cannot be attributed to a particular site adaptation method, so that other potential causes would need to be investigated, such as subjective user interventions or impacts of the specific training year selected for those methods.

KSI is a metric difficult to evaluate in general. Nevertheless, a general better performance can be observed in the three components by all QM-based methods as well as in SIMEQ (which uses an eQM procedure). Exceptions to this observation for some methods (CDF-T, KDM-R and QDM) may be found for Tamanrasset (due probably to unknown reasons beyond the methodology) and at very high-latitude sites. Obtaining any improvement at the three high-latitude sites is very challenging because their measured global irradiance can be positive at zero or negative sun elevation angles, and because the models selected for these sites where apparently highly uncertain.

Condensing the benchmarking and comparisons results in one unique and proper parameter might be questionable; however, in order to illustrate the results a unique metric called combined performance Index (CPI) can be used here (Gueymard, 2014). CPI is defined as a weighted sum of several metrics to combine information on the dispersion and on the distribution function similitude as well. That is,

$$CPI = (KSI + OVER + 2\,RMSE)/4. \tag{5}$$

Tables 4, 5 and 6 show the performance of the different site adaptation techniques for GHI, DNI and DHI, respectively, in terms of CPI (in percentage). In these tables, the row denoted as Raw Model and highlighted in bold refers to the original uncorrected model dataset. According to these results most methods resulted in improvement of the model datasets. There are, nevertheless, exceptions, such as the LIN-FIT method, that performs worse at Burns and at high-latitude sites. Despite the absence of any universal rule in the results, in several situations benefits can be obtained by separating the data into two subsets (clear and non-clear sky). In addition, the sequential use of methods, as occurs in the SIMEQ methodology, produces better performance. Quantile mapping based methodologies, in general, tend also to reduce the uncertainty.

Table 4. CPI (%) for GHI benchmarking results.

	ASP	**BOU**	**TAT**	**TAM**	**CAR**	**BRN**	**KIR**	**NRK**	**VIS**	**SBO**	**P50***
Raw Model	**25.5**	**54.0**	**23.7**	**39.7**	**25.2**	**46.0**	**138.1**	**91.5**	**92.3**	**45.6**	**45.8**
eQM-T	18.6	21.4	17.5	20.7	45.0	52.6	77.7	70.1	71.6	30.6	**37.8**
eQM-CS	19.3	20.4	17.7	20.3	46.3	52.9	72.3	54.4	57.4	22.7	**34.5**
KDM-T	24.5	23.4	21.2	20.9	48.2	36.7	78.1	70.8	72.6	36.6	**36.7**
KDM-CS	22.0	20.0	20.6	17.6	40.3	37.5	73.8	56.7	59.5	39.6	**38.6**
LIN-FIT	20.5	42.7	20.5	163.7	24.5	67.8	190.3	122.7	141.5	53.3	**60.6**
CDF-T	14.7	19.6	13.9	158.3	21.4	27.3	60.2	72.5	46.6	32.7	**30.0**
KDMR	20.6	19.2	12.5	155.4	16.7	33.8	51.6	43.3	49.2	29.5	**31.7**
QDM	12.9	21.2	15.8	177.8	17.6	30.1	48.4	51.2	63.8	34.9	**32.5**
SIM	9.8	55.2	27.3	25.1	17.8	70.2	109.6	75.9	49.4	12.1	**38.4**
SIMEQ	12.9	34.1	15.8	16.8	15.9	33.8	51.1	46.0	42.8	8.4	**25.3**
REG	71.5	37.6	21.0	76.8	109.4	59.2	97.5	71.5	79.1	101.5	**74.2**

*Median of CPI for all sites

Table 5. CPI (%) for DNI benchmarking results.

	ASP	BOU	TAT	TAM	CAR	BRN	KIR	NRK	VIS	SBO	P50*
Raw Model	**109.3**	**70.3**	**53.5**	**129.0**	**37.8**	**69.0**	**97.4**	**64.0**	**67.0**	**121.2**	**81.9**
eQM-T	58.3	36.4	28.3	32.8	42.3	62.5	90.8	67.1	68.5	33.6	**52.1**
eQM-CS	43.1	30.5	27.3	29.4	24.5	63.6	73.6	42.4	49.2	24.7	**40.8**
KDM-T	64.0	56.7	26.1	57.9	44.1	58.2	95.8	61.7	68.9	44.8	**57.8**
KDM-CS	56.7	30.7	22.0	34.8	40.2	53.4	71.1	39.6	49.7	36.1	**43.4**
LIN-FIT	80.7	118.9	31.2	54.5	50.2	131.5	93.8	129.0	123.4	94.6	**90.8**
CDF-T	40.0	40.0	26.9	76.5	47.1	49.6	65.9	56.6	153.5	48.1	**60.4**
KDMR	56.7	35.7	28.6	76.9	43.8	63.2	66.1	69.7	163.0	60.9	**66.5**
QDM	39.1	40.0	28.0	121.8	39.8	57.2	93.5	61.0	370.4	37.4	**88.8**
SIM	31.5	103.1	43.8	82.1	106.2	157.3	193.1	147.7	88.3	53.0	**100.6**
SIMEQ	21.4	54.5	35.5	30.6	31.0	41.0	78.7	53.5	49.5	18.5	**41.4**

*Median of CPI for all sites

Table 6. CPI for DHI benchmarking results.

	ASP	BOU	TAT	TAM	CAR	BRN	KIR	NRK	VIS	SBO	P50*
Raw Model	**83.0**	**68.2**	**69.1**	**123.8**	**89.7**	**150.8**	**83.4**	**84.8**	**86.2**	**193.8**	**103.3**
eQM-T	43.1	37.9	27.6	41.9	62.1	99.4	71.2	67.5	67.9	54.2	**57.3**
eQM-CS	29.4	36.0	27.1	34.4	55.5	94.9	71.0	64.6	64.4	43.4	**52.1**
KDM-T	39.3	41.3	22.8	42.6	68.8	82.5	70.3	66.5	67.9	52.1	**55.4**
KDM-CS	31.4	38.0	20.8	40.8	53.0	77.8	69.5	65.2	63.4	52.7	**51.3**
LIN-FIT	71.8	49.8	70.5	155.2	93.9	138.3	170.6	153.7	167.9	162.2	**123.4**
CDF-T	34.8	34.3	23.7	226.0	36.0	75.1	56.6	71.0	160.4	46.3	**76.4**
KDMR	36.5	37.4	28.3	133.2	43.3	74.4	58.0	51.5	142.7	43.0	**64.8**
QDM	31.5	37.4	26.5	415.9	40.7	81.3	63.3	59.0	214.9	45.5	**101.6**
SIM	63.4	103.8	53.6	96.8	141.6	119.4	144.3	110.7	144.1	77.3	**105.5**
SIMEQ	49.3	64.3	32.1	83.8	75.6	171.2	83.6	55.5	52.5	69.1	**73.7**

*Median of CPI for all sites

6. Sensitivity analysis

In addition to the benchmarking exercise, where the last complete year of ground measurements was used for training the improvement method, a sensitivity analysis on the training period was performed. This analysis was intended to determining the minimum period of time that should be used in the ground database for proper training. The sensitivity analysis has consisted in performing site adaptation to the 10 datasets of table 2 using the eQM-CS method with training periods of 3 months, 6 months, 1 year, 1.5 year and 2 years.

Figures 5 and 6 show the main statistical performance metrics for GHI and DNI (very similar results were found for DHI) compared to the uncorrected dataset referred to as model. It can be observed that a period of 3 months is insufficient to obtain significant improvement in most cases. Remarkably, such a short period tends to increase the KSI significantly, indicating that corrected data resulted in a worse similitude with the distribution function than the uncorrected data. For most of the cases, the sensitivity analysis indicates that 1-2 years of quality ground measurements are necessary to result in a general improvement of the solar radiation adapted data.

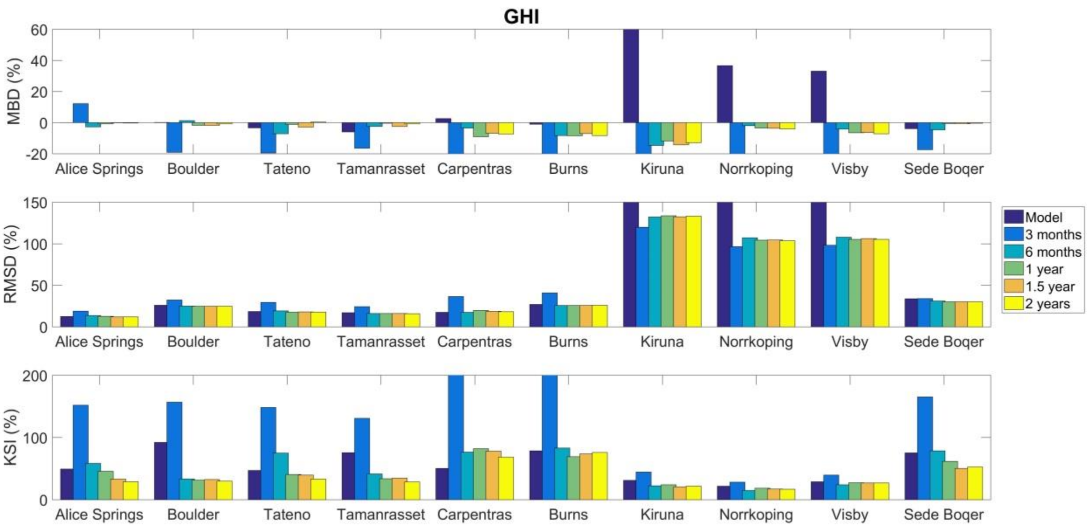

Figure 5. Sensitivity of GHI performance to the training period duration.

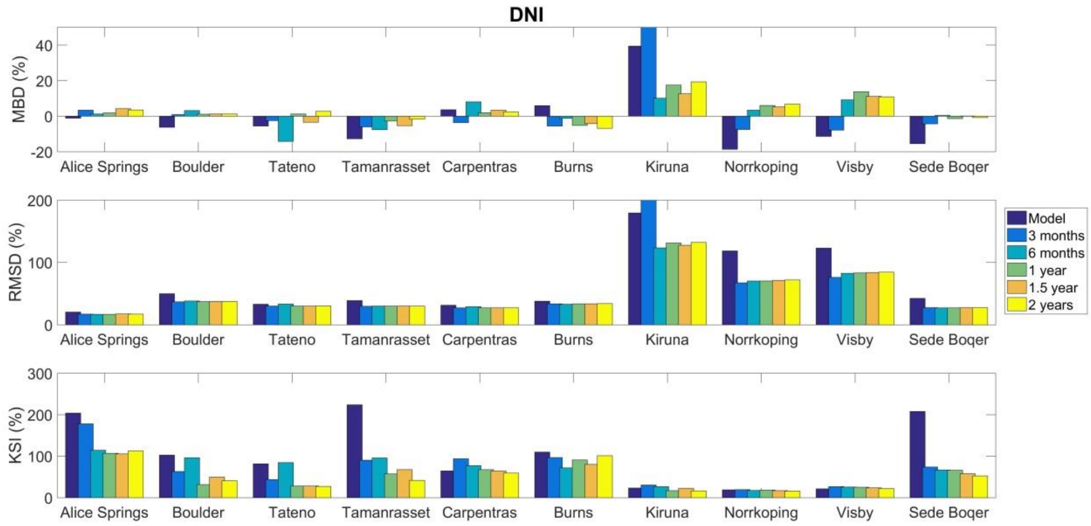

Figure 6. Sensitivity of DNI performance to the training period duration.

The sensitivity to a very large uncertainty in aerosol data (AOD, most importantly) or in the abundance of other atmospheric constituents in general can be also of interest, particularly for modeling DNI, which is the component strongly influenced by atmospheric aerosols and water vapor content in the atmosphere (Gueymard, 2012; Polo and Estalayo, 2015). The sensitivity analysis has been done by firstly generating satellite-derived DNI datasets for Carpentras, assuming different values (in terms of uncertainty in the atmospheric input) for the corresponding Linke turbidity factor. The latter's original estimated value at that site was adjusted in the range -30% to 30%. Assuming that the original TL value is perfectly true then the deviations can be considered as errors in the TL determination. Thus, regardless of the uncertainty in the original Linke turbidity factor, this sensitivity offers an assessment of the capability of site adaptation methods to correct situations with large overestimations or underestimations in atmospheric attenuating constituents. Here, the eQM-CS methodology was used for adapting or improving all the sensitivity cases. Figure 7 shows the sensitivity analysis results in terms of MBD, RMSD and KSI as a function of the assumed error in the TL value used as input to the satellite model. In this case a significant reduction in bias, dispersion and KSI is achieved by the correction method, even for very large over- and under-estimation of the atmospheric turbidity. Likewise, removal of substantial part of bias observed in DNI datasets with inaccurate aerosol information has been also reported in studies with other correction techniques (Gueymard, 2011; Gueymard et al., 2012).

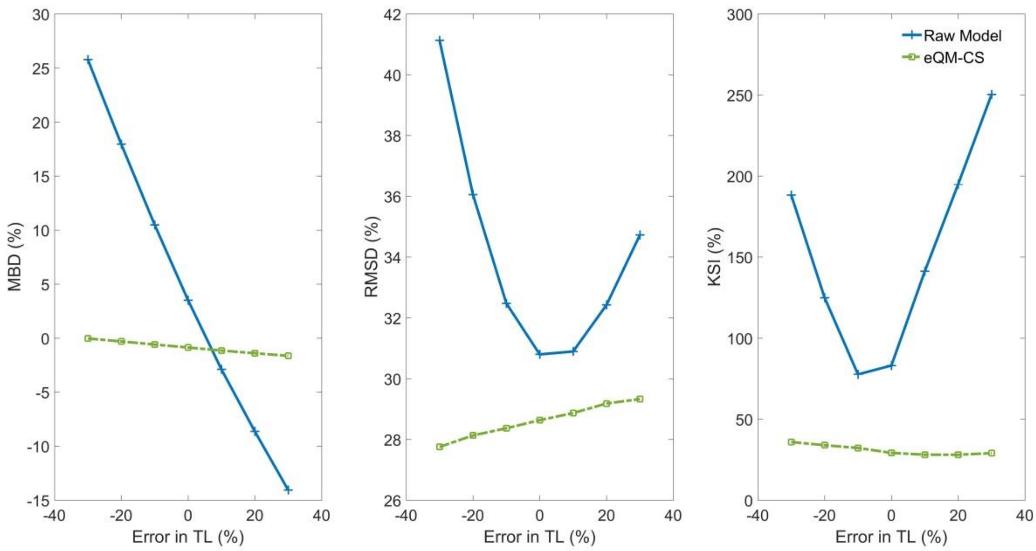

Figure 6. Sensitivity to the Linke turbidity uncertainty. Performance metrics of DNI for both the raw model and after correction with the eQM-CS method are shown.

7. Conclusion

Site adaptation of model-derived solar radiation time series is a general name for the procedure of correcting and improving long-term modeled datasets by comparing them to short-term overlapping ground measurements. Different methodologies can be used for adapting a dataset of solar irradiance components to a specific site. Some solar data suppliers have even developed their own methods. Many methodologies are also inspired by bias removal techniques used in other fields of meteorology and climatology. Two main families of methodologies can be identified according to the purpose of the correction: regression-like methods and quantile mapping, from which emerges also the combination of both as a third family. The former method focuses on fitting by linear or multiple regressions the modeled data with ground data to an equation able to be applied to the whole dataset. The quantile mapping techniques work on the probability domain and correct the solar radiation data by fitting the distribution function of modeled data to the distribution function of observational data.

Under the framework of IEA-PVPS Task 16 a benchmarking exercise of site adaptation techniques has been conducted by several participants in a blind exercise. Ten sites and ten different measured and modeled pairs of datasets were prepared to test ten different methods for site adaptation. Satellite-derived and reanalysis-based solar irradiance data were included in the tested datasets to expand the variety of modeled data as much as possible.

The results of this assessment of techniques have shown that most techniques are able to produce improvement and some degree of correction of modeled data. There are, however, situations where the quality of modeled data is already very high, so that it is hard to get noticeable improvement in the site-adapted data. Nevertheless, quantile mapping techniques have shown the potential of removing the bias observed in modeled data. In addition, specific strategies that disaggregate the datasets according to the state of the sky (clear, non-clear, ranges of clear-sky index, etc.) may offer better performance. Likewise, the proper combination of techniques, such as sequential use of multiple regression and quantile mapping, also resulted in significant improvement in most situations.

In addition, a sensitivity analysis has been performed to study the proper training period of ground data and the impact of very high bias in atmospheric input (AOD is frequently overestimated or underestimated in some regions with a potential detrimental impact on modeled solar radiation). Thus, it can be observed than ground-based data time series covering periods of at least about one year seems to be appropriate for proper training of adaptation methodologies at most sites. Moreover, for the case of high bias in AOD-related quantities, quantile mapping based methods have shown very good performance regardless of the uncertainty in the atmospheric information used as input.

Finally, it is worth mentioning that it is difficult to establish a universal method or procedure that works with the same efficacy in all possible combinations of sites and modeled datasets. Good-quality ground data are always highly recommended for proper training. Statistical methodologies can be very efficient in adapting modeled data to a reference one, but in real conditions the better the quality of the reference (ground data) the higher the potential improvement. Moreover, bad-quality measurements could actually result in biased site adaptations, possibly more biased than the original modeled dataset. In addition, a preliminary analysis of the uncertainty at the site under scrutiny could be recommended before selecting one method or another and before designing the proper subsets of data onto which the site adaptation methodologies would be applied. It must be also remarked that even though in this work we have shown mostly a pure statistical procedure it is recommended to adapt only GHI and DNI and to compute DHI in a way that ensures the consistency among the three components and the closure relation. In fact, this was the procedure followed by Team 3 with two of the methods. Besides, it should be pointed out that not all the correction methods have been tested in this work and, in this sense, more methodologies, as model output statistics (MOS) and others, should be investigated in future studies. The number and climatic diversity of sites used for testing should also be increased to obtain results as universal as possible.

Acknowledgements

This work constitutes the main contribution of several experts to the activity 2.2 of the Task 16 IEA-PVPS and Task V IEA-SolarPACES. The authors wish to acknowledge also the collaborative work and efforts carrying out by all the experts and participants in the task, both in this activity as in many others, contributing to increase the knowledge and applications of solar resource characterization.

References

Amillo, A., Huld, T., Müller, R., 2014. A New Database of Global and Direct Solar Radiation Using the Eastern Meteosat Satellite, Models and Validation. Remote Sensing 6, 8165–8189. doi:10.3390/rs6098165

Armansperg, M. v., Oechslin, D., Schweneke, M., 2015. Financial Modelling of PV Risks. Financial Modelling of Technical Risks in PV Projects.

Bright, J.M., Sun, X., Gueymard, C.A., Acord, B., Wang, P., Engerer, N.A., 2020. Bright-Sun: A globally applicable 1-min irradiance clear-sky detection model. Renewable and Sustainable Energy Reviews 121, 109706. doi:10.1016/j.rser.2020.109706

Cannon, A.J., 2018. Multivariate quantile mapping bias correction: an N-dimensional probability density function transform for climate model simulations of multiple variables. Climate Dynamics 50, 31–49. doi:10.1007/s00382-017-3580-6

Cannon, A.J., Sobie, S.R., Murdock, T.Q., 2015. Bias Correction of GCM Precipitation by Quantile Mapping. Journal of Climate 28, 6938–6959.

Cano, D., Monget, J.M.M., Albuisson, M., Guillard, H., Regas, N., Wald, L., 1986. A method for the determination of the global solar radiation from meteorological satellite data. Solar Energy 37, 31–39. doi:10.1016/0038-092X(86)90104-0

Carta, J.A., Velázquez, S., Cabrera, P., 2013. A review of measure-correlate-predict (MCP) methods used to estimate long-term wind characteristics at a target site. Renewable and Sustainable Energy Reviews. doi:10.1016/j.rser.2013.07.004

Cros, S., Turpin, M., Aillaud, P., Lallemand, C., 2019. Real-time solar irradiance retrieval from satellite data: quality assessment of an operational tool using five satellites, in: 6th International Conference Energy & Meteorology. Copenhagen (Denmark).

Déqué, M., Rowell, D.P., Lüthi, D., Giorgi, F., Christensen, J.H., Rockel, B., Jacob, D., Kjellström, E., de Castro, M., van den Hurk, B., 2007. An intercomparison of regional climate simulations for Europe: assessing uncertainties in model projections. Climatic Change 81, 53–70. doi:10.1007/s10584-006-9228-x

Feigenwinter, I., Kotlarski, S., Casanueva, A., Fischer, A.M., Schwierz, C., Liniger, M.A., 2018. Exploring quantile mapping as a tool to produce user-tailored climate scenarios for Switzerland. Technical Report MeteoSwiss, 270, 44 pp. 270.

Feng, F., Wang, K., 2019. Determining Factors of Monthly to Decadal Variability in Surface Solar Radiation in China: Evidences From Current Reanalyses. Journal of Geophysical Research: Atmospheres 124, 9161–9182. doi:10.1029/2018JD030214

Fernández-Peruchena, C.M., Vignola, F., Gastón, M., Lara-Fanego, V., Ramírez, L., Zarzalejo, L., Silva, M., Pavón, M., Moreno, S., Bermejo, D., Pulgar, J., Macias, S., Valenzuela, R.X., 2018. Probabilistic assessment of concentrated solar power plants yield: The EVA methodology. Renewable and Sustainable Energy Reviews 91, 802–811. doi:10.1016/j.rser.2018.03.018

Fernández Peruchena, C.M., Ramírez, L., Silva-Pérez, M.A., Lara, V., Bermejo, D., Gastón, M., Moreno-Tejera, S., Pulgar, J., Liria, J., Macías, S., Gonzalez, R., Bernardos, A., Castillo, N., Bolinaga, B., Valenzuela, R.X., Zarzalejo, L.F., 2016. A statistical characterization of the long-term solar resource: Towards risk assessment for solar power projects. Solar Energy 123, 29–39. doi:10.1016/j.solener.2015.10.051

Frank, C.W., Wahl, S., Keller, J.D., Pospichal, B., Hense, A., Crewell, S., 2018. Bias correction of a novel European reanalysis data set for solar energy applications. Solar Energy 164, 12–24. doi:10.1016/j.solener.2018.02.012

Guerreiro, L., Fernández-Peruchena, C.M., Cavaco, A., Gaston, M., Pereira, M.C., 2016. Experimental Validation of a Novel Methodology for Fast an Accurate Analysis of Solar Energy Yields Based on Cluster Analysis. Proceedings of EuroSun2016 1–8. doi:10.18086/eurosun.2016.09.03

Gueymard, C.A., 2011. Uncertainties in Modeled Direct Irradiance Around the Sahara as Affected by Aerosols: Are Current Datasets of Bankable Quality? Journal of Solar Energy Engineering 133, 031024, 1–13. doi:10.1115/1.4004386

Gueymard, C.A., 2012. Temporal variability in direct and global irradiance at various time scales as affected by aerosols. Solar Energy 86, 3544–3553. doi:10.1016/j.solener.2012.01.013

Gueymard, C.A., 2013. Aerosol turbidity derivation from broadband irradiance measurements: Methodological advances and uncertainty analysis. 42nd ASES National Solar Conference 2013, SOLAR 2013, Including 42nd ASES Annual Conference and 38th National Passive Solar Conference 637–644.

Gueymard, C.A., 2014. A review of validation methodologies and statistical performance indicators for modeled solar radiation data: Towards a better bankability of solar projects. Renewable and Sustainable Energy Reviews 39, 1024–1034. doi:10.1016/j.rser.2014.07.117

Gueymard, C.A., Bright, J.M., Lingfors, D., Habte, A., Sengupta, M., 2019. A posteriori clear-sky identification methods in solar irradiance time series: Review and preliminary validation using sky imagers. Renewable and Sustainable Energy Reviews 109, 412–427. doi:10.1016/J.RSER.2019.04.027

Gueymard, C.A., Gustafson, W.T., Bender, G., Etringer, A., Storck, P., 2012. Evaluation of procedures to improve solar resource assessments: Optimum use of short-term data from a local weather station to correct bias in long-term satellite derived solar radiation time series. World Renewable Energy Forum, WREF 2012, Including World Renewable Energy Congress XII and Colorado Renewable Energy Society (CRES) Annual Conferen 3, 2092–2099.

Hirsch, T., Dernsch, J., Fluri, T., García-Barberena, J., Giuliano, S., Hustig-Diethelm, F., Meyer, R., Schmidt, N., Seitz, M., Yildiz, E., 2017. SolarPACES Guideline for Bankable STE Yield Assessment. IEA Technology Collaboration Programme SolarPACES.

Huld, T., Paietta, E., Zangheri, P., Pinedo Pascua, I., 2018. Assembling Typical Meteorological Year Data Sets for Building Energy Performance Using Reanalysis and Satellite-Based Data. Atmosphere 9, 53. doi:10.3390/atmos9020053

Ines, A.V.M., Hansen, J.W., 2006. Bias correction of daily GCM rainfall for crop simulation studies. Agricultural and Forest Meteorology 138, 44–53. doi:10.1016/j.agrformet.2006.03.009

Izenman, A.J., 2016. Modern Multivariate Statistical Techniques : regression, classification, and manifold learning. Springer-Verlag New York.

Kothe, S., Hollmann, R., Pfeifroth, U., Träger-Chatterjee, C., Trentmann, J., Kothe, S., Hollmann, R., Pfeifroth, U., Träger-Chatterjee, C., Trentmann, J., 2019. The CM SAF R Toolbox—A Tool for the Easy Usage of Satellite-Based Climate Data in NetCDF Format. ISPRS International Journal of Geo-Information 8, 109. doi:10.3390/ijgi8030109

Lefèvre, M., Oumbe, A., Blanc, P., Espinar, B., Gschwind, B., Qu, Z., Wald, L., Schroedter-Homscheidt, M., Hoyer-Klick, C., Arola, A., Benedetti, A., Kaiser, J.W., Morcrette, J.-J., 2013. McClear: a new model estimating downwelling solar radiation at ground level in clear-sky conditions. Atmos. Meas. Tech 6, 2403–2418. doi:10.5194/amt-6-2403-2013

Long, C.N.N., Dutton, E.G.G., 2004. BSRN Global Network recommended QC tests, V2.0. BSRN Technical Report.

Mazorra Aguiar, L., Polo, J., Vindel, J.M.M., Oliver, A., 2019. Analysis of satellite derived solar irradiance in islands with site adaptation techniques for improving the uncertainty. Renewable Energy 135, 98–107. doi:10.1016/j.renene.2018.11.099

McGinnis, S., Nychka, D., Mearns, L.O., 2015. A New Distribution Mapping Technique for Climate Model Bias Correction, in: Machine Learning and Data Mining Approaches to Climate Science. Springer International Publishing, Cham, pp. 91–99. doi:10.1007/978-3-319-17220-0_9

Merrouni, A.A., Ghennioui, A., Wolfertstetter, F., Mezrhab, A., 2017. The uncertainty of the HelioClim-3 DNI data under Moroccan climate. AIP Conference Proceedings 1850, 140002–140011. doi:10.1063/1.4984519

Meyer, R., Schwandt, M., 2017. Documentation of Meteorological Data Sets delivered together with the SolarPACES Guideline for Bankable STE Yield Assessment, Version 2017. SolarPACES Report, www.solarpaces.org/yield-analysis-guideline.

Michelangeli, P.-A., Vrac, M., Loukos, H., 2009. Probabilistic downscaling approaches: Application to wind cumulative distribution functions. Geophysical Research Letters 36. doi:10.1029/2009GL038401

Molina, A., Falvey, M., Rondanelli, R., 2017. A solar radiation database for Chile. Scientific Reports 7, 14823. doi:10.1038/s41598-017-13761-x

Peng, X., She, J., Zhang, S., Tan, J., Li, Y., 2019. Evaluation of Multi-Reanalysis Solar Radiation Products Using Global Surface Observations. Atmosphere 10, 42. doi:10.3390/atmos10020042

Perdigão, J.C., Salgado, R., Costa, M.J., Dasari, H.P., Sanchez-Lorenzo, A., 2016. Variability and trends of downward surface global solar radiation over the Iberian Peninsula based on ERA-40 reanalysis. International Journal of Climatology 36, 3917–3933. doi:10.1002/joc.4603

Perez, R., Kivalov, S., Schlemmer, J., Hemker, K.J., Zelenka, A., 2010. Improving the performance of satellite-to-irradiance models using the satellite's infrared sensors. Proc. of American Solar Energy Society Annual Conference.

Perez, R., Schlemmer, J., Hemker, K., Kivalov, S., Kankiewicz, A., Gueymard, C., 2015. Satellite-to-Irradiance Modeling – A New Version of the SUNY Model, in: 42nd IEEE Photovoltaic Specialist Conference, At New Orleans, LA. doi:10.1109/PVSC.2015.7356212

Perez, R., Schlemmer, J., Kankiewicz, A., Dise, J., Tadese, A., Hoff, T., 2017. Detecting Calibration Drift at Reference Ground Truth Stations - A Demonstration of Satellite Irradiance Model's Accuracy, in: IEEE PVSC-44, Washington, DC.

Pfeifroth, U., Kothe, S., Müller, R., Trentmann, J., Hollmann, R., Fuchs, P., Werscheck, M., 2017. Surface Radiation Data Set - Heliosat (SARAH) - Edition 2. doi:10.5676/EUM_SAF_CM/SARAH/V002

Piani, C., Haerter, J.O., Coppola, E., 2010. Statistical bias correction for daily precipitation in regional climate models over Europe. Theoretical and Applied Climatology 99, 187–192. doi:10.1007/s00704-009-0134-9

Polo, J., Estalayo, G., 2015. Impact of atmospheric aerosol loads on Concentrating Solar Power production in arid-desert sites. Solar Energy 115, 621–631. doi:10.1016/j.solener.2015.03.031

Polo, J., Fernández-Peruchena, C., Gastón, M., 2017. Analysis on the long-term relationship between DNI and CSP yield production for different technologies. Solar Energy 115, 1121–1129. doi:10.1016/j.solener.2017.07.059

Polo, J., Martín, L., Vindel, J.M., 2015. Correcting satellite derived DNI with systematic and seasonal deviations: Application to India. Renewable Energy 80, 238–243. doi:http://dx.doi.org/10.1016/j.renene.2015.02.031

Polo, J., Perez, R., 2019. Solar radiation modeling from satellite imagery, in: Polo, J.; Martín-Pomares, L., Sanfilippo, A. (Ed.), Solar Resource Mapping - Fundamentals and Applications; Green Energy and Technology. Springer, pp. 183–197. doi:10.1007/978-3-319-97484-2_6

Polo, J., Téllez, F.M.M., Tapia, C., 2016a. Comparative analysis of long-term solar resource and CSP production for bankability. Renewable Energy 90, 38–45. doi:10.1016/j.renene.2015.12.057

Polo, J., Wilbert, S., Ruiz-Arias, J.A., Meyer, R., Gueymard, C., Súri, M., Martín, L., Mieslinger, T., Blanc, P., Grant, I., Boland, J., Ineichen, P., Remund, J., Escobar, R., Troccoli, A., Sengupta, M., Nielsen, K.P., Renne, D., Geuder, N., Cebecauer, T., 2016b. Preliminary survey on site-adaptation techniques for satellite-derived and reanalysis solar radiation datasets. Solar Energy 132, 25–37. doi:10.1016/j.solener.2016.03.001

Polo, J., Zarzalejo, L.F., Ramirez, L., 2008. Solar radiation derived from satellite images, Chap. 18. In: Modeling Solar Radiation at the Earth Surface, Chap. 18, in: Modeling Solar Radiation at the Earth Surface. Viorel Badescu. Springer-Verlag.

Porfirio, A.C.S., Ceballos, J.C., 2017. A method for estimating direct normal irradiation from GOES geostationary satellite imagery: Validation and application over Northeast Brazil. doi:10.1016/j.solener.2017.05.096

Posselt, R., Mueller, R.W., Stöckli, R., Trentmann, J., 2012. Remote sensing of solar surface radiation for climate monitoring - the CM-SAF retrieval in international comparison. Remote Sensing of Environment 118, 186–198. doi:10.1016/j.rse.2011.11.016

Qu, Z., Gschwind, B., Lefevre, M., Wald, L., Oumbe, A., Blanc, P., Espinar, B., Gesell, G., Gschwind, B., Klüser, L., Lefèvre, M., Saboret, L., Schroedter-Homscheidt, M., Wald, L., 2017. Fast radiative transfer parameterisation for assessing the surface solar irradiance: The Heliosat-4 method. Meteorologische Zeitschrift 26, 33–57. doi:10.1127/metz/2016/0781

Ramirez Camargo, L., Dorner, W., 2016. Comparison of satellite imagery based data, reanalysis data and statistical methods for mapping global solar radiation in the Lerma Valley (Salta, Argentina). Renewable Energy 99, 57–68. doi:10.1016/j.renene.2016.06.042

Remund, J., Ramirez, L., Wilbert, S., Blanc, P., Lorenz, E., Köhler, C., Renné, D., 2017. Solar Resource for High Penetration and Large Scale Applications - A New Joint Task of IEA PVPS and IEA SolarPACES, in: Amsterdam, N. (Ed.), 33rd European Photovoltaic Solar Energy Conference and Exhibition PVSEC. pp. 14–15. doi:DOI: 10.4229/EUPVSEC20172017-6BV.3.2

Richter, M., Kalisch, J., Schmidt, T., Lorenz, E., De Brabandere, K., 2015. Best Practice Guide On Uncertainty in PV Modelling.

Riihelä, A., 2018. Validation of the SARAH-E Satellite-Based Surface Solar Radiation Estimates over India. Remote Sensing 10, 1–16. doi:10.3390/rs10030392

Salazar, G., Gueymard, C., Galdino, J.B., de Castro Vilela, O., Fraidenraich, N., 2020. Solar irradiance time series derived from high-quality measurements, satellite-based models, and reanalyses at a near-equatorial site in Brazil. Renewable and Sustainable Energy Reviews 117. doi:10.1016/j.rser.2019.109478

Sengupta, M., Habte, A., Gueymard, C., Wilbert, S., Renné, D., 2017. Best Practices Handbook for the Collection and Use of Solar Resource Data for Solar Energy Applications: Second Edition. doi:10.18777/ieashc-task46-2015-0001

Sengupta, M., Xie, Y., Lopez, A., Habte, A., Maclaurin, G., Shelby, J., 2018. The National Solar Radiation Data Base (NSRDB). Renewable and Sustainable Energy Reviews 89, 51–60. doi:10.1016/J.RSER.2018.03.003

Tahir, Z. ul R., Azhar, M., Blanc, P., Asim, M., Imran, S., Hayat, N., Shahid, H., Ali, H., 2020. The evaluation of reanalysis and analysis products of solar radiation for Sindh province, Pakistan. Renewable Energy 145, 347–362. doi:10.1016/j.renene.2019.04.107

Tang, W., Qin, J., Yang, K., Liu, S., Lu, N., Niu, X., 2016. Retrieving high-resolution surface solar radiation with cloud parameters derived by combining MODIS and MTSAT data. Atmospheric Chemistry and Physics 16, 2543–2557. doi:10.5194/acp-16-2543-2016

Themeßl, M.J., Gobiet, A., Heinrich, G., 2012. Empirical-statistical downscaling and error correction of regional climate models and its impact on the climate change signal. Climatic Change 112, 449–468. doi:10.1007/s10584-011-0224-4

Thomas, C., Saboret, L., Wey, E., Blanc, P., Wald, L., 2016. Validation of the new HelioClim-3 version 4 real-time and short-term forecast service using 14 BSRN stations. Advances in Science and Research 13, 129–136. doi:10.5194/asr-13-129-2016

Trolliet, M., Walawender, J.P., Bourlès, B., Boilley, A., Trentmann, J., Blanc, P., Lefèvre, M., Wald, L., 2018. Downwelling surface solar irradiance in the tropical Atlantic Ocean: a comparison of re-analyses and satellite-derived data sets to PIRATA measurements. Ocean Science 14, 1021–1056. doi:10.5194/os-14-1021-2018

Urraca, R., Gracia-Amillo, A.M., Huld, T., Martinez-De-Pison, F.J., Trentmann, J., Lindfors, A. V, Riihelä, A., Sanz-Garcia, A., 2017. Quality control of global solar radiation data with satellite-based products. doi:10.1016/j.solener.2017.09.032

Urraca, R., Huld, T., Gracia-Amillo, A., Martinez-de-Pison, F.J., Kaspar, F., Sanz-Garcia, A., 2018. Evaluation of global horizontal irradiance estimates from ERA5 and COSMO-REA6 reanalyses using ground and satellite-based data. Solar Energy 164, 339–354. doi:10.1016/J.SOLENER.2018.02.059

Wilcke, R.A.I., Mendlik, T., Gobiet, A., 2013. Multi-variable error correction of regional climate models. Climatic Change 120, 871–887. doi:10.1007/s10584-013-0845-x

Yang, D., 2018. A correct validation of the National Solar Radiation Data Base (NSRDB). Renewable and Sustainable Energy Reviews 97, 152–155. doi:10.1016/J.RSER.2018.08.023

Yang, D., 2019. Post-processing of NWP forecasts using ground or satellite-derived data through kernel conditional density estimation. Journal of Renewable and Sustainable Energy 11, 026101. doi:10.1063/1.5088721

Yang, D., Boland, J., 2019. Satellite-augmented diffuse solar radiation separation models. Journal of Renewable and Sustainable Energy 11, 023705. doi:10.1063/1.5087463

Yang, D., Perez, R., 2019. Can we gauge forecasts using satellite-derived solar irradiance? Journal of Renewable and Sustainable Energy 11, 023704. doi:10.1063/1.5087588

Zib, B.J., Dong, X., Xi, B., Kennedy, A., 2012. Evaluation and Intercomparison of Cloud Fraction and Radiative Fluxes in Recent Reanalyses over the Arctic Using BSRN Surface Observations. Journal of Climate 25, 2291–2305. doi:10.1175/JCLI-D-11-00147.1